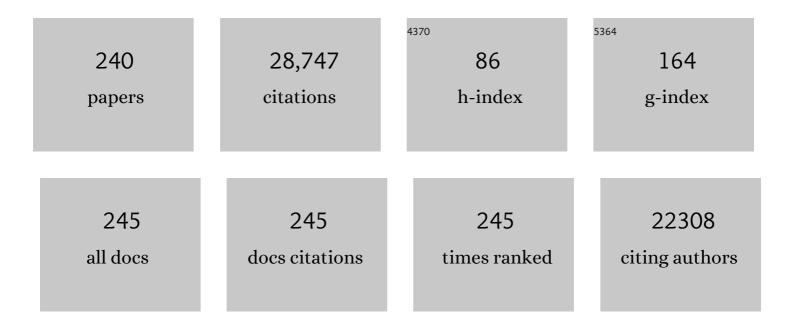
C Daniel Frisbie

List of Publications by Year in descending order

Source: https://exaly.com/author-pdf/4662557/publications.pdf Version: 2024-02-01



#	Article	lF	CITATIONS
1	Introduction to Organic Thin Film Transistors and Design of n-Channel Organic Semiconductors. Chemistry of Materials, 2004, 16, 4436-4451.	3.2	1,256
2	Printable ion-gel gate dielectrics for low-voltage polymer thin-film transistorsÂonÂplastic. Nature Materials, 2008, 7, 900-906.	13.3	1,077
3	Functional Group Imaging by Chemical Force Microscopy. Science, 1994, 265, 2071-2074.	6.0	988
4	Electrolyteâ€Gated Transistors for Organic and Printed Electronics. Advanced Materials, 2013, 25, 1822-1846.	11.1	797
5	Electrical Resistance of Long Conjugated Molecular Wires. Science, 2008, 320, 1482-1486.	6.0	663
6	Critical assessment of charge mobility extraction in FETs. Nature Materials, 2018, 17, 2-7.	13.3	571
7	Fabrication and Characterization of Metalâ^'Moleculeâ^'Metal Junctions by Conducting Probe Atomic Force Microscopy. Journal of the American Chemical Society, 2001, 123, 5549-5556.	6.6	539
8	Transition from Direct Tunneling to Field Emission in Metal-Molecule-Metal Junctions. Physical Review Letters, 2006, 97, 026801.	2.9	526
9	Chemical Force Microscopy: Exploiting Chemically-Modified Tips To Quantify Adhesion, Friction, and Functional Group Distributions in Molecular Assemblies. Journal of the American Chemical Society, 1995, 117, 7943-7951.	6.6	523
10	Length-Dependent Transport in Molecular Junctions Based on SAMs of Alkanethiols and Alkanedithiols:Â Effect of Metal Work Function and Applied Bias on Tunneling Efficiency and Contact Resistance. Journal of the American Chemical Society, 2004, 126, 14287-14296.	6.6	493
11	Electrostatic modification of novel materials. Reviews of Modern Physics, 2006, 78, 1185-1212.	16.4	465
12	Distance Dependence of Electron Tunneling through Self-Assembled Monolayers Measured by Conducting Probe Atomic Force Microscopy:  Unsaturated versus Saturated Molecular Junctions. Journal of Physical Chemistry B, 2002, 106, 2813-2816.	1.2	461
13	Highâ€Resolution Patterning of Graphene by Screen Printing with a Silicon Stencil for Highly Flexible Printed Electronics. Advanced Materials, 2015, 27, 109-115.	11.1	430
14	Ion Gel Gated Polymer Thin-Film Transistors. Journal of the American Chemical Society, 2007, 129, 4532-4533.	6.6	422
15	Structural Characterization of a Pentacene Monolayer on an Amorphous SiO2Substrate with Grazing Incidence X-ray Diffraction. Journal of the American Chemical Society, 2004, 126, 4084-4085.	6.6	412
16	Organic Thin Film Transistors Based onN-Alkyl Perylene Diimides:Â Charge Transport Kinetics as a Function of Gate Voltage and Temperature. Journal of Physical Chemistry B, 2004, 108, 19281-19292.	1.2	406
17	"Cut and Stick―Rubbery Ion Gels as High Capacitance Gate Dielectrics. Advanced Materials, 2012, 24, 4457-4462.	11.1	383
18	Contact Resistance in Metalâ^'Moleculeâ^'Metal Junctions Based on Aliphatic SAMs:  Effects of Surface Linker and Metal Work Function, Journal of the American Chemical Society, 2002, 124, 11268-11269	6.6	372

#	Article	IF	CITATIONS
19	Printed, Sub-3V Digital Circuits on Plastic from Aqueous Carbon Nanotube Inks. ACS Nano, 2010, 4, 4388-4395.	7.3	362
20	Electronic Impurity Doping in CdSe Nanocrystals. Nano Letters, 2012, 12, 2587-2594.	4.5	335
21	Ion Gel-Gated Polymer Thin-Film Transistors: Operating Mechanism and Characterization of Gate Dielectric Capacitance, Switching Speed, and Stability. Journal of Physical Chemistry C, 2009, 113, 8972-8981.	1.5	325
22	Effect of Dielectric Roughness on Performance of Pentacene TFTs and Restoration of Performance with a Polymeric Smoothing Layer. Journal of Physical Chemistry B, 2005, 109, 10574-10577.	1.2	305
23	Gravure Printing of Graphene for Largeâ€area Flexible Electronics. Advanced Materials, 2014, 26, 4533-4538.	11.1	298
24	Formation of Metalâ^'Moleculeâ^'Metal Tunnel Junctions:Â Microcontacts to Alkanethiol Monolayers with a Conducting AFM Tip. Journal of the American Chemical Society, 2000, 122, 2970-2971.	6.6	296
25	Optimization of Aerosol Jet Printing for High-Resolution, High-Aspect Ratio Silver Lines. ACS Applied Materials & Interfaces, 2013, 5, 4856-4864.	4.0	296
26	Gated four-probe measurements on pentacene thin-film transistors: Contact resistance as a function of gate voltage and temperature. Journal of Applied Physics, 2004, 96, 7312-7324.	1.1	288
27	Correlation between HOMO Alignment and Contact Resistance in Molecular Junctions:Â Aromatic Thiols versus Aromatic Isocyanides. Journal of the American Chemical Society, 2006, 128, 4970-4971.	6.6	282
28	Surface potential profiling and contact resistance measurements on operating pentacene thin-film transistors by Kelvin probe force microscopy. Applied Physics Letters, 2003, 83, 5539-5541.	1.5	277
29	A π-Stacking Terthiophene-Based Quinodimethane Is an n-Channel Conductor in a Thin Film Transistor. Journal of the American Chemical Society, 2002, 124, 4184-4185.	6.6	275
30	Measuring Relative Barrier Heights in Molecular Electronic Junctions with Transition Voltage Spectroscopy. ACS Nano, 2008, 2, 827-832.	7.3	254
31	Polymer Electrolyte-Gated Organic Field-Effect Transistors:  Low-Voltage, High-Current Switches for Organic Electronics and Testbeds for Probing Electrical Transport at High Charge Carrier Density. Journal of the American Chemical Society, 2007, 129, 6599-6607.	6.6	251
32	Molecular Tunnel Junctions Based on π-Conjugated Oligoacene Thiols and Dithiols between Ag, Au, and Pt Contacts: Effect of Surface Linking Group and Metal Work Function. Journal of the American Chemical Society, 2011, 133, 19864-19877.	6.6	247
33	Molecular Rectification in a Metalâ~'Insulatorâ~'Metal Junction Based on Self-Assembled Monolayers. Journal of the American Chemical Society, 2002, 124, 11730-11736.	6.6	232
34	Field Effect Transport and Trapping in Regioregular Polythiophene Nanofibers. Journal of Physical Chemistry B, 2004, 108, 19169-19179.	1.2	232
35	Systems for orthogonal self-assembly of electroactive monolayers on Au and ITO: an approach to molecular electronics. Journal of the American Chemical Society, 1995, 117, 6927-6933.	6.6	231
36	Solution Processable, Electrochromic Ion Gels for Sub-1 V, Flexible Displays on Plastic. Chemistry of Materials, 2015, 27, 1420-1425.	3.2	219

#	Article	IF	CITATIONS
37	Transition from Tunneling to Hopping Transport in Long, Conjugated Oligo-imine Wires Connected to Metals. Journal of the American Chemical Society, 2010, 132, 4358-4368.	6.6	217
38	Low-voltage operation of a pentacene field-effect transistor with a polymer electrolyte gate dielectric. Applied Physics Letters, 2005, 86, 103503.	1.5	215
39	Imaging of features on surfaces by condensation figures. Science, 1993, 260, 647-649.	6.0	212
40	Aerosol Jet Printed, Low Voltage, Electrolyte Gated Carbon Nanotube Ring Oscillators with Sub-5 μs Stage Delays. Nano Letters, 2013, 13, 954-960.	4.5	207
41	Conducting Probe Atomic Force Microscopy: A Characterization Tool for Molecular Electronics. Advanced Materials, 1999, 11, 261-264.	11.1	204
42	p-Channel Organic Semiconductors Based on Hybrid Aceneâ^'Thiophene Molecules for Thin-Film Transistor Applications. Journal of the American Chemical Society, 2005, 127, 3997-4009.	6.6	204
43	Solution-Processable Electrochemiluminescent Ion Gels for Flexible, Low-Voltage, Emissive Displays on Plastic. Journal of the American Chemical Society, 2014, 136, 3705-3712.	6.6	204
44	Multicolored, Low-Power, Flexible Electrochromic Devices Based on Ion Gels. ACS Applied Materials & Interfaces, 2016, 8, 6252-6260.	4.0	202
45	Variable temperature film and contact resistance measurements on operatingn-channel organic thin film transistors. Journal of Applied Physics, 2004, 95, 6396-6405.	1.1	190
46	lonic Conductivity, Capacitance, and Viscoelastic Properties of Block Copolymer-Based Ion Gels. Macromolecules, 2011, 44, 940-949.	2.2	183
47	Nanoporous Poly(3-alkylthiophene) Thin Films Generated from Block Copolymer Templates. Macromolecules, 2008, 41, 67-75.	2.2	182
48	Printed Subâ€⊋ V Gelâ€Electrolyteâ€Gated Polymer Transistors and Circuits. Advanced Functional Materials, 2010, 20, 587-594.	7.8	180
49	High Toughness, High Conductivity Ion Gels by Sequential Triblock Copolymer Self-Assembly and Chemical Cross-Linking. Journal of the American Chemical Society, 2013, 135, 9652-9655.	6.6	177
50	Polymer Electrolyte Gate Dielectric Reveals Finite Windows of High Conductivity in Organic Thin Film Transistors at High Charge Carrier Densities. Journal of the American Chemical Society, 2005, 127, 6960-6961.	6.6	175
51	Electrolyte-gated transistors for enhanced performance bioelectronics. Nature Reviews Methods Primers, 2021, 1, .	11.8	172
52	Exploiting Ionic Coupling in Electronic Devices: Electrolyteâ€Gated Organic Fieldâ€Effect Transistors. Advanced Materials, 2008, 20, 3177-3180.	11.1	170
53	Scalable, Selfâ€Aligned Printing of Flexible Graphene Microâ€5upercapacitors. Advanced Energy Materials, 2017, 7, 1700285.	10.2	167
54	Electrical Impedance of Spin-Coatable Ion Gel Films. Journal of Physical Chemistry B, 2011, 115, 3315-3321.	1.2	166

#	Article	IF	CITATIONS
55	Probing Hopping Conduction in Conjugated Molecular Wires Connected to Metal Electrodes. Chemistry of Materials, 2011, 23, 631-645.	3.2	163
56	Temperature and Length Dependence of Charge Transport in Redox-Active Molecular Wires Incorporating Ruthenium(II) Bis(Ïf-arylacetylide) Complexes. Journal of Physical Chemistry C, 2007, 111, 7521-7526.	1.5	161
57	Correlation of Phase Behavior and Charge Transport in Conjugated Polymer/Fullerene Blends. Journal of Physical Chemistry C, 2008, 112, 17726-17736.	1.5	156
58	Direct Force Measurements at Polymer Brush Surfaces by Atomic Force Microscopy. Macromolecules, 1998, 31, 4297-4300.	2.2	155
59	Photosensitive Self-Assembled Monolayers on Gold: Photochemistry of Surface-Confined Aryl Azide and Cyclopentadienylmanganese Tricarbonyl. Journal of the American Chemical Society, 1994, 116, 4395-4404.	6.6	153
60	Hopping transport and the Hall effect near the insulator–metal transition in electrochemically gated poly(3-hexylthiophene) transistors. Nature Communications, 2012, 3, 1210.	5.8	153
61	Experimental and Theoretical Analysis of Nanotransport in Oligophenylene Dithiol Junctions as a Function of Molecular Length and Contact Work Function. ACS Nano, 2015, 9, 8022-8036.	7.3	152
62	Gate Voltage Dependent Resistance of a Single Organic Semiconductor Grain Boundary. Journal of Physical Chemistry B, 2001, 105, 4538-4540.	1.2	143
63	Rubrene-Based Single-Crystal Organic Semiconductors: Synthesis, Electronic Structure, and Charge-Transport Properties. Chemistry of Materials, 2013, 25, 2254-2263.	3.2	141
64	Comparison of the Mobility–Carrier Density Relation in Polymer and Singleâ€Crystal Organic Transistors Employing Vacuum and Liquid Gate Dielectrics. Advanced Materials, 2009, 21, 2174-2179.	11.1	140
65	Printed, subâ€2V ZnO Electrolyte Gated Transistors and Inverters on Plastic. Advanced Materials, 2013, 25, 3413-3418.	11.1	140
66	Electrolyte Gate-Controlled Kondo Effect in <mml:math xmlns:mml="http://www.w3.org/1998/Math/MathML" display="inline"><mml:msub><mml:mi>SrTiO</mml:mi><mml:mn>3</mml:mn></mml:msub>. Physical Review Letters, 2011, 107, 256601.</mml:math 	2.9	139
67	Field effect conductance of conducting polymer nanofibers. Journal of Polymer Science, Part B: Polymer Physics, 2003, 41, 2674-2680.	2.4	136
68	Temperature and gate voltage dependent transport across a single organic semiconductor grain boundary. Journal of Applied Physics, 2001, 90, 1342-1349.	1.1	135
69	Size-Dependent Electrical Transport in CdSe Nanocrystal Thin Films. Nano Letters, 2010, 10, 3727-3732.	4.5	134
70	Temperatureâ€Independent Transport in Highâ€Mobility Dinaphthoâ€Thienoâ€Thiophene (DNTT) Single Crystal Transistors. Advanced Materials, 2013, 25, 3478-3484.	11.1	133
71	Allâ€Printed, Foldable Organic Thinâ€Film Transistors on Glassine Paper. Advanced Materials, 2015, 27, 7058-7064.	11.1	133
72	Potentiometry of an operating organic semiconductor field-effect transistor. Applied Physics Letters, 2001, 78, 993-995.	1.5	119

5

#	Article	IF	CITATIONS
73	Performance and Stability of Aerosol-Jet-Printed Electrolyte-Gated Transistors Based on Poly(3-hexylthiophene). ACS Applied Materials & Interfaces, 2013, 5, 6580-6585.	4.0	116
74	High-Resolution Transfer Printing of Graphene Lines for Fully Printed, Flexible Electronics. ACS Nano, 2017, 11, 7431-7439.	7.3	116
75	Size- and Temperature-Dependent Charge Transport in PbSe Nanocrystal Thin Films. Nano Letters, 2011, 11, 3887-3892.	4.5	114
76	Screen Printing of Highly Loaded Silver Inks on Plastic Substrates Using Silicon Stencils. ACS Applied Materials & Interfaces, 2015, 7, 12619-12624.	4.0	114
77	High Carrier Densities Achieved at Low Voltages in Ambipolar PbSe Nanocrystal Thin-Film Transistors. Nano Letters, 2009, 9, 3848-3852.	4.5	111
78	Length and Temperature Dependent Conduction of Ruthenium-Containing Redox-Active Molecular Wires. Journal of Physical Chemistry C, 2011, 115, 19955-19961.	1.5	104
79	Vibrational Spectroscopy Reveals Electrostatic and Electrochemical Doping in Organic Thin Film Transistors Gated with a Polymer Electrolyte Dielectric. Journal of the American Chemical Society, 2007, 129, 7824-7830.	6.6	100
80	Viscoelastic Properties, Ionic Conductivity, and Materials Design Considerations for Poly(styrene- <i>b</i> -ethylene oxide- <i>b</i> -styrene)-Based Ion Gel Electrolytes. Macromolecules, 2011, 44, 8981-8989.	2.2	97
81	Dependence of Conductivity on Charge Density and Electrochemical Potential in Polymer Semiconductors Gated with Ionic Liquids. Journal of Physical Chemistry C, 2012, 116, 3132-3141.	1.5	94
82	Single Ion Conducting, Polymerized Ionic Liquid Triblock Copolymer Films: High Capacitance Electrolyte Gates for n-type Transistors. ACS Applied Materials & Interfaces, 2015, 7, 7294-7302.	4.0	93
83	Analysis of the Causes of Variance in Resistance Measurements on Metalâ~'Moleculeâ~'Metal Junctions Formed by Conducting-Probe Atomic Force Microscopy. Journal of Physical Chemistry B, 2005, 109, 16801-16810.	1.2	92
84	High charge carrier densities and conductance maxima in single-crystal organic field-effect transistors with a polymer electrolyte gate dielectric. Applied Physics Letters, 2006, 88, 203504.	1.5	91
85	Aerosol Jet Printed, Subâ€2 V Complementary Circuits Constructed from <i>P</i> ―and <i>N</i> â€Type Electrolyte Gated Transistors. Advanced Materials, 2014, 26, 7032-7037.	11.1	90
86	Determination of Energy-Level Alignment in Molecular Tunnel Junctions by Transport and Spectroscopy: Self-Consistency for the Case of Oligophenylene Thiols and Dithiols on Ag, Au, and Pt Electrodes. Journal of the American Chemical Society, 2019, 141, 3670-3681.	6.6	90
87	Synergistic Increase in Ionic Conductivity and Modulus of Triblock Copolymer Ion Gels. Macromolecules, 2015, 48, 4942-4950.	2.2	89
88	Tetracene air-gap single-crystal field-effect transistors. Applied Physics Letters, 2007, 90, 162106.	1.5	85
89	Ultralow contact resistance in electrolyte-gated organic thin film transistors. Applied Physics Letters, 2010, 97, .	1.5	85
90	Field Effect Conductance Measurements on Thin Crystals of Sexithiophene. Journal of Physical Chemistry B, 1999, 103, 8842-8849.	1.2	83

#	Article	IF	CITATIONS
91	Enhanced Hopping Conductivity in Low Band Gap Donorâ^Acceptor Molecular Wires Up to 20 nm in Length. Journal of the American Chemical Society, 2010, 132, 16191-16201.	6.6	82
92	Length-Dependent Conductance of Conjugated Molecular Wires Synthesized by Stepwise "Click― Chemistry. Journal of the American Chemical Society, 2010, 132, 8854-8855.	6.6	81
93	Organic Electrical Double Layer Transistors Based on Rubrene Single Crystals: Examining Transport at High Surface Charge Densities above 10 ¹³ cm ^{–2} . Journal of Physical Chemistry C, 2011, 115, 14360-14368.	1.5	81
94	Electrostatic <i>versus</i> Electrochemical Doping and Control of Ferromagnetism in Ion-Gel-Gated Ultrathin La _{0.5} Sr _{0.5} CoO _{3â^îr} . ACS Nano, 2016, 10, 7799-7810.	7.3	81
95	Field Effect Transport Measurements on Single Grains of Sexithiophene:Â Role of the Contacts. Journal of Physical Chemistry B, 2000, 104, 12202-12209.	1.2	80
96	Grain Orientation Mapping of Polycrystalline Organic Semiconductor Films by Transverse Shear Microscopy. Advanced Materials, 2008, 20, 4033-4039.	11.1	80
97	Surface Potential Mapping of SAMâ€Functionalized Organic Semiconductors by Kelvin Probe Force Microscopy. Advanced Materials, 2011, 23, 502-507.	11.1	78
98	Length-Dependent Nanotransport and Charge Hopping Bottlenecks in Long Thiophene-Containing Ï€-Conjugated Molecular Wires. Journal of the American Chemical Society, 2015, 137, 15732-15741.	6.6	76
99	Investigation of Charge Transport in Thin, Doped Sexithiophene Crystals by Conducting Probe Atomic Force Microscopy. Journal of Physical Chemistry B, 1998, 102, 1679-1688.	1.2	75
100	Strain effects on the work function of an organic semiconductor. Nature Communications, 2016, 7, 10270.	5.8	74
101	Aerosol Jet Printed p- and n-type Electrolyte-Gated Transistors with a Variety of Electrode Materials: Exploring Practical Routes to Printed Electronics. ACS Applied Materials & Interfaces, 2014, 6, 18704-18711.	4.0	73
102	Carrier Localization on Surfaces of Organic Semiconductors Gated with Electrolytes. Physical Review Letters, 2010, 105, 036802.	2.9	71
103	High-Mobility Transistors Based on Single Crystals of Isotopically Substituted Rubrene- <i>d</i> ₂₈ . Journal of Physical Chemistry C, 2013, 117, 11522-11529.	1.5	71
104	Transport properties of single-crystal tetracene field-effect transistors with silicon dioxide gate dielectric. Applied Physics Letters, 2004, 85, 422-424.	1.5	69
105	Scanning electron microscopy for imaging photopatterned self-assembled monolayers on gold. Langmuir, 1993, 9, 1517-1520.	1.6	68
106	Energy Level Alignment in Molecular Tunnel Junctions by Transport and Spectroscopy: Self-Consistency for the Case of Alkyl Thiols and Dithiols on Ag, Au, and Pt Electrodes. Journal of the American Chemical Society, 2019, 141, 18182-18192.	6.6	68
107	Comparison of DC and AC Transport in 1.5–7.5 nm Oligophenylene Imine Molecular Wires across Two Junction Platforms: Eutectic Ga–In versus Conducting Probe Atomic Force Microscope Junctions. Journal of the American Chemical Society, 2016, 138, 7305-7314.	6.6	64
108	N- and P-Channel Transport Behavior in Thin Film Transistors Based on Tricyanovinyl-Capped Oligothiophenes. Journal of Physical Chemistry B, 2006, 110, 14590-14597.	1.2	63

#	Article	IF	CITATIONS
109	Enhancement of the Morphology and Open Circuit Voltage in Bilayer Polymer/Fullerene Solar Cells. Journal of Physical Chemistry C, 2009, 113, 11408-11415.	1.5	63
110	Label-Free DNA Sensing Platform with Low-Voltage Electrolyte-Gated Transistors. Analytical Chemistry, 2015, 87, 1861-1866.	3.2	63
111	Correlation of on-state conductance with referenced electrochemical potential in ion gel gated polymer transistors. Applied Physics Letters, 2009, 94, 013304.	1.5	60
112	Uncovering a law of corresponding states for electron tunneling in molecular junctions. Nanoscale, 2015, 7, 10465-10471.	2.8	60
113	A Pedagogical Perspective on Ambipolar FETs. ChemPhysChem, 2013, 14, 1547-1552.	1.0	59
114	Transfer Printing of Thermoreversible Ion Gels for Flexible Electronics. ACS Applied Materials & Interfaces, 2013, 5, 9522-9527.	4.0	56
115	Utilizing Carbon Nanotube Electrodes to Improve Charge Injection and Transport in Bis(trifluoromethyl)-dimethyl-rubrene Ambipolar Single Crystal Transistors. ACS Nano, 2013, 7, 10245-10256.	7.3	56
116	Charge Transport in 4 nm Molecular Wires with Interrupted Conjugation: Combined Experimental and Computational Evidence for Thermally Assisted Polaron Tunneling. ACS Nano, 2016, 10, 4372-4383.	7.3	56
117	Crystal step edges can trap electrons on the surfaces of n-type organic semiconductors. Nature Communications, 2018, 9, 2141.	5.8	55
118	Hydrostatic-pressure dependence of the photoconductivity of single-crystal pentacene and tetracene. Applied Physics Letters, 2001, 79, 2731-2733.	1.5	54
119	Synthesis, Optical Properties, and Microstructure of a Fullerene-Terminated Poly(3-hexylthiophene). Macromolecules, 2009, 42, 4118-4126.	2.2	54
120	Highâ€Transconductance Organic Thinâ€Film Electrochemical Transistors for Driving Lowâ€Voltage Redâ€Greenâ€Blue Active Matrix Organic Lightâ€Emitting Devices. Advanced Functional Materials, 2012, 22, 1623-1631.	7.8	54
121	Effect of Heteroatom Substitution on Transport in Alkanedithiol-Based Molecular Tunnel Junctions: Evidence for Universal Behavior. ACS Nano, 2017, 11, 569-578.	7.3	54
122	The Catalytic Mechanics of Dynamic Surfaces: Stimulating Methods for Promoting Catalytic Resonance. ACS Catalysis, 2020, 10, 12666-12695.	5.5	54
123	Direct Detection by Atomic Force Microscopy of Single Bond Forces Associated with the Rupture of Discrete Charge-Transfer Complexes. Journal of the American Chemical Society, 2002, 124, 15125-15133.	6.6	53
124	DC-Driven, Sub-2 V Solid-State Electrochemiluminescent Devices by Incorporating Redox Coreactants into Emissive Ion Gels. Chemistry of Materials, 2014, 26, 5358-5364.	3.2	52
125	Relationship between Diode Saturation Current and Open Circuit Voltage in Poly(3-alkylthiophene) Solar Cells as a Function of Device Architecture, Processing Conditions, and Alkyl Side Chain Length. Journal of Physical Chemistry C, 2011, 115, 20806-20816.	1.5	51
126	Influence of Silver Doping on Electron Transport in Thin Films of PbSe Nanocrystals. Advanced Materials, 2013, 25, 725-731.	11.1	51

#	Article	IF	CITATIONS
127	Effects of Olefin Content and Alkyl Chain Placement on Optoelectronic and Morphological Properties in Poly(thienylene vinylenes). Macromolecules, 2013, 46, 5184-5194.	2.2	50
128	Rapid, Selective, Label-Free Aptameric Capture and Detection of Ricin in Potable Liquids Using a Printed Floating Gate Transistor. ACS Sensors, 2016, 1, 1213-1216.	4.0	50
129	Hydrostatic pressure dependence of charge carrier transport in single-crystal rubrene devices. Applied Physics Letters, 2005, 86, 123501.	1.5	49
130	Why one can expect large rectification in molecular junctions based on alkane monothiols and why rectification is so modest. Chemical Science, 2018, 9, 4456-4467.	3.7	49
131	Work function and temperature dependence of electron tunneling through an N-type perylene diimide molecular junction with isocyanide surface linkers. Nanoscale, 2018, 10, 964-975.	2.8	49
132	Subâ€3 V ZnO Electrolyteâ€Gated Transistors and Circuits with Screenâ€Printed and Photo rosslinked Ion Gel Gate Dielectrics: New Routes to Improved Performance. Advanced Functional Materials, 2020, 30, 1902028.	7.8	49
133	Diastereoselectivity of Enolate Anion Protonation. H/D Exchange of β-Substituted Ethyl Butanoates in Ethanol-d. Journal of the American Chemical Society, 1997, 119, 479-486.	6.6	48
134	Electrochemiluminescent displays based on ion gels: correlation between device performance and choice of electrolyte. Journal of Materials Chemistry C, 2016, 4, 8448-8453.	2.7	48
135	Gate-Tuned Insulator–Metal Transition in Electrolyte-Gated Transistors Based on Tellurene. Nano Letters, 2019, 19, 4738-4744.	4.5	48
136	Detection of Discrete Interactions upon Rupture of Au Microcontacts to Self-Assembled Monolayers Terminated with â^'S(CO)CH3or â^'SH. Journal of the American Chemical Society, 2000, 122, 9750-9760.	6.6	47
137	Rupture of Hydrophobic Microcontacts in Water:Â Correlation of Pull-Off Force with AFM Tip Radius. Langmuir, 2000, 16, 6294-6297.	1.6	47
138	Low Band Gap Poly(thienylene vinylene)/Fullerene Bulk Heterojunction Photovoltaic Cells. Journal of Physical Chemistry C, 2009, 113, 10790-10797.	1.5	47
139	Operating and Sensing Mechanism of Electrolyte-Gated Transistors with Floating Gates: Building a Platform for Amplified Biodetection. Journal of Physical Chemistry C, 2016, 120, 108-117.	1.5	46
140	Exceptionally Small Statistical Variations in the Transport Properties of Metal–Molecule–Metal Junctions Composed of 80 Oligophenylene Dithiol Molecules. Journal of the American Chemical Society, 2017, 139, 5696-5699.	6.6	45
141	HOMO Level Pinning in Molecular Junctions: Joint Theoretical and Experimental Evidence. Journal of Physical Chemistry Letters, 2018, 9, 2394-2403.	2.1	45
142	Simultaneous Nanoindentation and Electron Tunneling through Alkanethiol Self-Assembled Monolayers. Journal of Physical Chemistry B, 2006, 110, 10011-10020.	1.2	44
143	A Selfâ€Aligned Strategy for Printed Electronics: Exploiting Capillary Flow on Microstructured Plastic Surfaces. Advanced Electronic Materials, 2015, 1, 1500137.	2.6	43
144	Observation of Unusual Homoepitaxy in Ultrathin Pentacene Films and Correlation with Surface Electrostatic Potential. Advanced Materials, 2009, 21, 3092-3098.	11.1	41

#	Article	IF	CITATIONS
145	An ADMET Route to Low-Band-Gap Poly(3-hexadecylthienylene vinylene): A Systematic Study of Molecular Weight on Photovoltaic Performance. Macromolecules, 2012, 45, 2190-2199.	2.2	41
146	Printable, Degradable, and Biocompatible Ion Gels from a Renewable ABA Triblock Polyester and a Low Toxicity Ionic Liquid. ACS Macro Letters, 2017, 6, 1083-1088.	2.3	41
147	Growth of ultrathin pentacene films on polymeric substrates. Physical Review B, 2009, 80, .	1.1	40
148	Band Gap and HOMO Level Control in Poly(thienylene vinylene)s Prepared by ADMET Polymerization. ACS Macro Letters, 2012, 1, 986-990.	2.3	40
149	Aerosol-Jet-Printed, 1 Volt H-Bridge Drive Circuit on Plastic with Integrated Electrochromic Pixel. ACS Applied Materials & Interfaces, 2013, 5, 13198-13206.	4.0	40
150	Parasitic Capacitance Effect on Dynamic Performance of Aerosol-Jet-Printed Sub 2 V Poly(3-hexylthiophene) Electrolyte-Gated Transistors. ACS Applied Materials & Interfaces, 2016, 8, 27012-27017.	4.0	40
151	Field Effect Modulation of Electrocatalytic Hydrogen Evolution at Back-Gated Two-Dimensional MoS ₂ Electrodes. Nano Letters, 2019, 19, 6118-6123.	4.5	40
152	Polylactideâ^'Polythiopheneâ^'Polylactide Triblock Copolymers. Macromolecules, 2010, 43, 3566-3569.	2.2	39
153	Determination of Quasi-Fermi Levels across Illuminated Organic Donor/Acceptor Heterojunctions by Kelvin Probe Force Microscopy. Journal of the American Chemical Society, 2011, 133, 13802-13805.	6.6	39
154	High Conductance 2D Transport around the Hall Mobility Peak in Electrolyte-Gated Rubrene Crystals. Physical Review Letters, 2014, 113, 246602.	2.9	39
155	High-Resolution, High-Aspect Ratio Conductive Wires Embedded in Plastic Substrates. ACS Applied Materials & Interfaces, 2015, 7, 1841-1847.	4.0	39
156	2D Insulator–Metal Transition in Aerosolâ€Jetâ€Printed Electrolyteâ€Gated Indium Oxide Thin Film Transistors. Advanced Electronic Materials, 2017, 3, 1600369.	2.6	38
157	Currentâ^'Voltage Hysteresis and Memory Effects in Ambipolar Organic Thin Film Transistors Based on a Substituted Oligothiophene. Journal of Physical Chemistry C, 2007, 111, 452-456.	1.5	37
158	Photoswitchable Hopping Transport in Molecular Wires 4 nm in Length. Journal of Physical Chemistry C, 2016, 120, 6442-6449.	1.5	37
159	Use of high lateral resolution secondary-ion mass spectrometry to characterize self-assembled monolayers on microfabricated structures. Journal of the American Chemical Society, 1992, 114, 7142-7145.	6.6	36
160	Pentacene organic field-effect transistor on metal substrate with spin-coated smoothing layer. Applied Physics Letters, 2004, 85, 4406.	1.5	36
161	Conducting channel formation and annihilation in organic field-effect structures. Journal of Applied Physics, 2009, 105, .	1.1	35
162	Transfer Printing of Sub-5 μm Graphene Electrodes for Flexible Microsupercapacitors. ACS Applied Materials & Interfaces, 2018, 10, 22303-22310.	4.0	34

#	Article	IF	CITATIONS
163	Electrolyte gated single-crystal organic transistors to examine transport in the high carrier density regime. MRS Bulletin, 2013, 38, 43-50.	1.7	33
164	Printed, Selfâ€Aligned Sideâ€Gate Organic Transistors with a Subâ€5 µm Gate–Channel Distance on Imprinted Plastic Substrates. Advanced Electronic Materials, 2016, 2, 1600293.	2.6	33
165	All-Printed, Self-Aligned Carbon Nanotube Thin-Film Transistors on Imprinted Plastic Substrates. ACS Applied Materials & Interfaces, 2018, 10, 15926-15932.	4.0	33
166	High Lateral Resolution Imaging by Secondary Ion Mass Spectrometry of Photopatterned Self-Assembled Monolayers Containing Aryl Azide. Langmuir, 1995, 11, 2563-2571.	1.6	32
167	Length Dependence of Charge Transport in Nanoscopic Molecular Junctions Incorporating a Series of Rigid Thiol-Terminated Norbornylogs. Journal of Physical Chemistry B, 2005, 109, 5207-5215.	1.2	32
168	Hopping Transport and Rectifying Behavior in Long Donor–Acceptor Molecular Wires. Journal of Physical Chemistry C, 2014, 118, 26485-26497.	1.5	32
169	Negative Isotope Effect on Fieldâ€Effect Hole Transport in Fully Substituted ¹³ Câ€Rubrene. Advanced Electronic Materials, 2017, 3, 1700018.	2.6	32
170	High Capacitance, Photo-Patternable Ion Gel Gate Insulators Compatible with Vapor Deposition of Metal Gate Electrodes. ACS Applied Materials & Interfaces, 2014, 6, 19275-19281.	4.0	30
171	Detection and Sourcing of Gluten in Grain with Multiple Floating-Gate Transistor Biosensors. ACS Sensors, 2018, 3, 395-402.	4.0	30
172	Self-Assembled Monolayers with Charge-Transfer Functional Groups:Â Immobilization of the Electron Donor TMPD and the Electron Acceptor TCNQ. Langmuir, 1998, 14, 5834-5840.	1.6	29
173	Determination of Quantum Capacitance and Band Filling Potential in Graphene Transistors with Dual Electrochemical and Field-Effect Gates. Journal of Physical Chemistry C, 2014, 118, 21160-21169.	1.5	29
174	Hydrostatic-pressure dependence of organic thin-film transistor current versus voltage characteristics. Applied Physics Letters, 2004, 85, 5760-5762.	1.5	27
175	Field Effect Modulation of Heterogeneous Charge Transfer Kinetics at Back-Gated Two-Dimensional MoS ₂ Electrodes. Nano Letters, 2017, 17, 7586-7592.	4.5	27
176	Freestanding Ion Gels for Flexible, Printed, Multifunctional Microsupercapacitors. ACS Applied Materials & Interfaces, 2019, 11, 9947-9954.	4.0	27
177	Examination of Au, Cu, and Al contacts in organic field-effect transistors via displacement current measurements. Journal of Applied Physics, 2011, 110, .	1.1	26
178	Wettability Contrast Gravure Printing. Advanced Materials, 2015, 27, 7420-7425.	11.1	26
179	Field Effect Modulation of Outer-Sphere Electrochemistry at Back-Gated, Ultrathin ZnO Electrodes. Journal of the American Chemical Society, 2016, 138, 7220-7223.	6.6	26
180	Characterization of the Electric Double Layer Formation Dynamics of a Metal/Ionic Liquid/Metal Structure. ACS Applied Materials & amp; Interfaces, 2016, 8, 14879-14884.	4.0	25

#	Article	IF	CITATIONS
181	Quantifying Molecular Structure-Tunneling Conductance Relationships: Oligophenylene Dimethanethiol vs Oligophenylene Dithiol Molecular Junctions. Journal of Physical Chemistry C, 2021, 125, 4292-4298.	1.5	25
182	Lithium Perchlorate-Doped Poly(styrene- <i>b</i> -ethylene oxide- <i>b</i> -styrene) Lamellae-Forming Triblock Copolymer as High Capacitance, Smooth, Thin Film Dielectric. Journal of Physical Chemistry C, 2009, 113, 3903-3908.	1.5	24
183	Designing a robust single-molecule switch. Science, 2016, 352, 1394-1395.	6.0	24
184	Thin Film Transistors Based on Alkylphenyl Quaterthiophenes:Â Structure and Electrical Transport Properties. Chemistry of Materials, 2007, 19, 1355-1361.	3.2	23
185	Contact Mechanics Modeling of Pull-Off Measurements:Â Effect of Solvent, Probe Radius, and Chemical Binding Probability on the Detection of Single-Bond Rupture Forces by Atomic Force Microscopy. Analytical Chemistry, 2002, 74, 3096-3104.	3.2	22
186	Negative magnetoresistance of organic field effect transistors. Applied Physics Letters, 2007, 91, .	1.5	21
187	High Open-Circuit Voltage Photovoltaic Cells with a Low Bandgap Copolymer of Isothianaphthene, Thiophene, and Benzothiadiazole Units. Journal of Physical Chemistry C, 2009, 113, 21928-21936.	1.5	21
188	Synthesis, Solid State Properties, and Semiconductor Measurements of 5,6,11,12-Tetrachlorotetracene. Journal of Physical Chemistry C, 2009, 113, 16544-16548.	1.5	21
189	Facile Method for Fabricating Flexible Substrates with Embedded, Printed Silver Lines. ACS Applied Materials & Interfaces, 2014, 6, 1306-1312.	4.0	21
190	Charge Density Dependent Twoâ€Channel Conduction in Organic Electric Double Layer Transistors (EDLTs). Advanced Materials, 2014, 26, 2527-2532.	11.1	21
191	Electric-field effect on photoluminescence of lead-halide perovskites. Materials Today, 2019, 28, 31-39.	8.3	21
192	Mechanical Deformation Distinguishes Tunneling Pathways in Molecular Junctions. Journal of the American Chemical Society, 2019, 141, 497-504.	6.6	21
193	Site-specific chemical doping reveals electron atmospheres at the surfaces of organic semiconductor crystals. Nature Materials, 2021, 20, 1532-1538.	13.3	21
194	Structural and vibrational characterization of the organic semiconductor tetracene as a function of pressure and temperature. Chemical Physics, 2006, 325, 138-151.	0.9	20
195	Large Magnetoresistance at Room Temperature in Organic Molecular Tunnel Junctions with Nonmagnetic Electrodes. ACS Nano, 2016, 10, 8571-8577.	7.3	20
196	Interfacial Charge Contributions to Chemical Sensing by Electrolyte-Gated Transistors with Floating Gates. Journal of Physical Chemistry Letters, 2018, 9, 1335-1339.	2.1	19
197	Printed, 1 V electrolyte-gated transistors based on poly(3-hexylthiophene) operating at >10 kHz on plastic. Applied Physics Letters, 2018, 113, .	1.5	19
198	Microfluidic opportunities in printed electrolyte-gated transistor biosensors. Biomicrofluidics, 2020, 14, 011301.	1.2	19

#	Article	IF	CITATIONS
199	Fabrication of a Sexithiophene Semiconducting Wire: Nanoshaving with an Atomic Force Microscope Tip. Advanced Materials, 2000, 12, 285-288.	11.1	18
200	Intramolecular Exciton Diffusion in Poly(3-hexylthiophene). Journal of Physical Chemistry Letters, 2013, 4, 3445-3449.	2.1	18
201	Self-aligned inkjet printing of resistors and low-pass resistor–capacitor filters on roll-to-roll imprinted plastics with resistances ranging from 10 to 10 ⁶ Ω. Flexible and Printed Electronics, 2018, 3, 045003.	1.5	18
202	Growth of Thin, Anisotropic, π-Conjugated Molecular Films by Stepwise "Click―Assembly of Molecular Building Blocks: Characterizing Reaction Yield, Surface Coverage, and Film Thickness versus Addition Step Number. Journal of the American Chemical Society, 2015, 137, 8819-8828.	6.6	17
203	High-Resolution, High-Aspect-Ratio Printed and Plated Metal Conductors Utilizing Roll-to-Roll Microscale UV Imprinting with Prototype Imprinting Stamps. Industrial & Engineering Chemistry Research, 2018, 57, 16335-16346.	1.8	17
204	Hopping Conductance in Molecular Wires Exhibits a Large Heavy-Atom Kinetic Isotope Effect. Journal of the American Chemical Society, 2021, 143, 2638-2643.	6.6	17
205	Mixing at the Charged Interface of a Polymer Semiconductor and a Polyelectrolyte Dielectric. Journal of Physical Chemistry Letters, 2010, 1, 862-867.	2.1	15
206	Electronic Polarization at Pentacene/Polymer Dielectric Interfaces: Imaging Surface Potentials and Contact Potential Differences as a Function of Substrate Type, Growth Temperature, and Pentacene Microstructure. Journal of Physical Chemistry C, 2014, 118, 2487-2497.	1.5	15
207	Charge Saturation and Intrinsic Doping in Electrolyte-Gated Organic Semiconductors. Journal of Physical Chemistry Letters, 2015, 6, 4840-4844.	2.1	15
208	Continuous and Reversible Tuning of Electrochemical Reaction Kinetics on Back-Gated 2D Semiconductor Electrodes: Steady-State Analysis Using a Hydrodynamic Method. Analytical Chemistry, 2019, 91, 1627-1635.	3.2	15
209	Inkjet-printed, self-aligned organic Schottky diodes on imprinted plastic substrates. Flexible and Printed Electronics, 2020, 5, 015006.	1.5	15
210	Transient effects controlling the charge carrier population of organic field effect transistor channels. Journal of Applied Physics, 2010, 107, .	1.1	14
211	Self-aligned capillarity-assisted printing of top-gate thin-film transistors on plastic. Flexible and Printed Electronics, 2018, 3, 035004.	1.5	13
212	Tuning of HOMO energy levels and open circuit voltages in solar cells based on statistical copolymers prepared by ADMET polymerization. Polymer Chemistry, 2014, 5, 6287-6294.	1.9	12
213	Quantitative Surface Coverage Measurements of Self-Assembled Monolayers by Nuclear Reaction Analysis of Carbon-12. Journal of Physical Chemistry Letters, 2016, 7, 3477-3481.	2.1	12
214	Optimized dielectric properties of SrTiO3:Nbâ^•SrTiO3 (001) films for high field effect charge densities. Applied Physics Letters, 2006, 89, 242915.	1.5	11
215	Single Crystal Field Effect Transistor of a Y-Shaped Ladder-Type Oligomer. Journal of Physical Chemistry C, 2008, 112, 7968-7971.	1.5	11
216	Sub-Band Filling, Mott-like Transitions, and Ion Size Effects in C ₆₀ Single Crystal Electric Double Layer Transistors. ACS Nano, 2022, 16, 4823-4830.	7.3	10

#	Article	IF	CITATIONS
217	Extended 7,7,8,8-Tetracyano- <i>p</i> -quinodimethane-Based Acceptors: How Molecular Shape and Packing Impact Electron Accepting Behavior. Crystal Growth and Design, 2009, 9, 4599-4601.	1.4	9
218	Coupling of channel conductance and gate-to-channel capacitance in electric double layer transistors. Applied Physics Letters, 2013, 103, 193304.	1.5	9
219	Measuring the Thickness and Potential Profiles of the Space-Charge Layer at Organic/Organic Interfaces under Illumination and in the Dark by Scanning Kelvin Probe Microscopy. ACS Applied Materials & Interfaces, 2016, 8, 5772-5776.	4.0	9
220	Quantitative analysis of weak current rectification in molecular tunnel junctions subject to mechanical deformation reveals two different rectification mechanisms for oligophenylene thiols <i>versus</i> alkane thiols. Nanoscale, 2021, 13, 16755-16768.	2.8	9
221	Alumina Graphene Catalytic Condenser for Programmable Solid Acids. Jacs Au, 2022, 2, 1123-1133.	3.6	9
222	Scanning Kelvin Probe Microscopy Reveals Planar Defects Are Sources of Electronic Disorder in Organic Semiconductor Crystals. Advanced Electronic Materials, 2017, 3, 1700117.	2.6	8
223	Self-Aligned Capillarity-Assisted Printing of High Aspect Ratio Flexible Metal Conductors: Optimizing Ink Flow, Plating, and Mechanical Adhesion. Industrial & Engineering Chemistry Research, 2020, 59, 22107-22122.	1.8	8
224	Strain–Work Function Relationship in Single-Crystal Tetracene. ACS Applied Materials & Interfaces, 2020, 12, 40607-40612.	4.0	7
225	Synthesis, X-ray, spectroelectrochemical, and theoretical studies of a tricyanovinyl-capped quaterthiophene: A correlation of semiconductor performance with physical properties. Chemical Physics Letters, 2006, 425, 251-256.	1.2	6
226	Rubrene Single-Crystal Transistors with Perfluoropolyether Liquid Dielectric: Exploiting Free Dipoles to Induce Charge Carriers at Organic Surfaces. Journal of Physical Chemistry C, 2017, 121, 6540-6545.	1.5	6
227	Theory of magnetoresistance of organic molecular tunnel junctions with nonmagnetic electrodes. Physical Review B, 2017, 95, .	1.1	6
228	Open-channel microfluidic diodes based on two-tier junctions. Applied Physics Letters, 2018, 113, .	1.5	6
229	Quantifying Image Charge Effects in Molecular Tunnel Junctions Based on Self-Assembled Monolayers of Substituted Oligophenylene Ethynylene Dithiols. ACS Applied Materials & Interfaces, 2021, 13, 56404-56412.	4.0	6
230	Sub-3 V, MHz-Class Electrolyte-Gated Transistors and Inverters. ACS Applied Materials & Interfaces, 2022, 14, 21295-21300.	4.0	6
231	Charge carrier extraction dynamics for organic field effect transistor structures. Applied Physics Letters, 2011, 99, 073306.	1.5	5
232	Detection and amplification of capacitance- and charge-based signals using printed electrolyte gated transistors with floating gates. Flexible and Printed Electronics, 2019, 4, 044001.	1.5	5
233	Modeling of Quasi-Static Floating-Gate Transistor Biosensors. ACS Sensors, 2021, 6, 1910-1917.	4.0	4
234	Solution-based, additive fabrication of flush metal conductors in plastic substrates by printing and plating in two-level capillary channels. Flexible and Printed Electronics, 2021, 6, 045005.	1.5	3

#	Article	IF	CITATIONS
235	Transistors: Aerosol Jet Printed, Sub-2 V Complementary Circuits Constructed fromP- andN-Type Electrolyte Gated Transistors (Adv. Mater. 41/2014). Advanced Materials, 2014, 26, 7131-7131.	11.1	2
236	Anomalous Cooling-Rate-Dependent Charge Transport in Electrolyte-Gated Rubrene Crystals. Journal of Physical Chemistry Letters, 2018, 9, 4828-4833.	2.1	2
237	Transient Charge Carrier Transport Effects in Organic Field Effect Transistor Channels. Materials Research Society Symposia Proceedings, 2010, 1270, 1.	0.1	1
238	Homoepitaxial growth modes in textured, polycrystalline ultrathin pentacene films on dielectrics. Physica Status Solidi (B): Basic Research, 2015, 252, 1291-1299.	0.7	1
239	Electrical Characterization of Thin Single Crystals of Sexithiophene. Materials Research Society Symposia Proceedings, 1997, 488, 431.	0.1	0
240	Tapping Mode Near-Field Scanning Optical Microscopy of Molecular Crystals and Thin Films. Microscopy and Microanalysis, 1999, 5, 994-995.	0.2	0